

Probabilistic Machine Learning for Detection of Tightening Torque in Bolted Joints

Journal Title
XX(X):1–17
©The Author(s) 2020
Reprints and permission:
sagepub.co.uk/journalsPermissions.nav
DOI: 10.1177/ToBeAssigned
www.sagepub.com/

SAGE

Luccas Miguel¹ , Rafael Teloli¹ , Samuel da Silva¹  and Gaël Chevallier²

Abstract

Observing the loss of tightening torque using modal parameters is challenging due to the variability and nonlinear effects in bolted joints. Thus, this paper proposes a combined application of two probabilistic machine learning methods. First, a Gaussian mixture model (GMM) is learned using estimated natural frequencies, assuming the tightening torque in a safe situation. This probabilistic model can assuredly detect the lack of torque using indirect vibration measures in other unknown states by computing a damage index. A Gaussian process regression (GPR) is also learned considering a set of torque and damage index pairs in several conditions. The GPR model interpolates a curve to supply an estimative of the tightening torque for other conditions not used in this learning. An illustrative application is performed considering the Orion beam, an academic-scale specimen composed of a lap-joint configuration that retains the friction surface in contact patches. The structure is subjected to a random vibration with a controlled RMS level and several tightening torque conditions to identify the modal parameters. The probabilistic model learning via the GMM and GPR can detect adequately, with a low number of false diagnoses, the actual state of torque using an indirect measure of vibration, i.e., without the need for a torque sensor on each bolt.

Keywords

bolted joints, tightening torque, probabilistic machine learning, Gaussian mixture model, Gaussian process regression

Introduction

One of the most utilized forms to connect structures is by using bolted joints; besides ensuring safe and stiffness to the structural systems, the presence of joints offers the possibility of building complex systems with modular geometry, which often facilitates the replacement of damaged components by healthy counterparts. Thus, it stands out that the use of joints in an industrial context is gaining more attention, with applications ranging from aero and wind turbines (Chou et al., 2018, Siewert et al., 2010) to bolted-flange joints in oil and gas plants (Reza et al., 2014). Notwithstanding the advantages behind such a design strategy, locations containing bolted joints are susceptible to structural damages (small cracks may propagate Qiu et al. (2014)). In contrast, bolt loosening is commonly seen when the structure is subject to external vibration sources (Doyle et al., 2010, Li and Jing, 2017, Oregui et al., 2017). Due to these reasons, many methods are proposed for monitoring the health of bolted joints (Miao et al., 2020, Wang et al., 2013a), and this work focuses on approaches for the detection of torque conditions in bolts.

The literature suggests organizing these approaches into two categories based on the instrumentation used (Nikraves and Goudarzi, 2017). The first one includes the direct methods. Each bolt or a set of joints is monitored using specific sensors, typically employing strain gauges or load cells to estimate information about the stress state and then compare it with the design requirements. The key idea is to assess an empirical relationship of bolt loosening using

the stress-torque in each bolted joint. The most popular algorithm is the torque wrench method (Motosh, 1976). However, a significant fluctuation is expected using this approach induced by numerous uncertainties (Nazarko and Ziemianski, 2017). Thus, discrepancies affect the accuracy of loosening detection, limiting its use in widespread applications. Another limitation is that many structures with bolted joints, such as pipes, are submerged or in complex human access regions for regular inspection (Razi et al., 2013). This category trend involves using an automated computer-vision method combined with machine learning algorithms to estimate the bolted joints' tightening level (Cha et al., 2016, Ramana et al., 2019).

The second category of approaches is using indirect methods. Active sensing approaches using piezoelectric sensors/actuators are attractive and regularly used for detecting torque loosening in this class, mainly applying electromechanical impedance (Park et al., 2001, Wang et al., 2013b). Machine learning algorithms have been using

¹UNESP - Universidade Estadual Paulista, Departamento de Engenharia Mecânica, Av. Brasil 56, 15385-000, Ilha Solteira - SP, Brazil

²Institut FEMTO-ST, Département Mécanique Appliquée, UBFC - Université de Bourgogne Franche-Comté, Besançon, France

Corresponding author:

Samuel da Silva, UNESP - Universidade Estadual Paulista, Departamento de Engenharia Mecânica, Av. Brasil 56, 15385-000, Ilha Solteira - SP, Brazil.

Email: samuel.silva13@unesp.br

electromechanical signatures to propose new extraction features for computing damage index with classification, for example, adopting a support vector machine method (Wang et al., 2020). However, vibration-based data is still the most prevalent approach (Milanese et al., 2008).

Razi et al. (2013) suggest using empirical mode decomposition as a useful energy-based damage index assuming tests performed in a pipeline's bolted flange joint with progressive torque loss. In this class of approach, induced vibration can be collected using a piezoceramic actuator (Wang and Song, 2019), impact modulations (Meyer and Adams, 2019), or shakers with harmonic excitations (Li and Jing, 2020). Features extracted from the spectrum transmissibility are typically used to diagnose the level of tightening torque (Li and Jing, 2020).

Modal parameters are standard features extracted from these spectrum signatures due to consolidated identification methods in commercial software. On the other hand, these parameters are essential linear features. Consequently, the sensitivity to robustly detect small changes in tightening torque of lap-joints is still a challenge, once diverse nonlinear mechanisms may appear due to interactions between assembled components, as hysteretic damping induced by friction, dynamic clearance, and other effects (Segalman, 2006); To the best of our knowledge, the best safe detection of lack of tightening torque currently present in the literature is in the order of approximately ten times less than a torque condition considered healthy (Luo and Yu, 2017). An effective way to treat the inherent nonlinearities seems to be by applying a higher-order spectrum, as the Volterra series (Villani et al., 2020).

Luo and Yu (2017) proposed a new method for damage identification of structures with bolted joints based on a residual error of the Auto-Regressive model in time series analysis. In this particular work, the authors could only observe torque changes when the undamaged condition's level reduced from 20 Nm to 2.5 Nm in the damaged one. Although significant changes in torque values do not imply equal proportions in the dynamics of jointed structures, at this level, the assembled components are practical without any connection and with great severity of variation. Another critical point that lacks investigation is to define the degree of damage severity due to loss of tightening without having a direct torque measurement embedded at each bolted joint. The proposal to have a simple and clear indicator to quantify this value is of interest to the industry. Consequently, the use of modal properties in bolted joints to characterize and quantify damage and be used in stochastic SHM strategies is still open in the literature.

In this sense, this paper's main contribution lies in proposing an integrated approach based on machine learning techniques but with a physical interpretation on the detection of tightening torque problems. From the frequency spectrum of vibration signals, model features are estimated to implement a Gaussian Mixture Model (GMM) to classification and a Gaussian Process Regression (GPR) to quantify torque values in a testbed of an Orion beam.

The benchmark proposed by Teloli et al. (2021) is an academic-scale specimen that provides controlled tightening torque conditions on the bolts that comprise the lap-joint. Nevertheless, the structure exhibits dynamic behavior typical to other bolted joint systems (Brake, 2018). At first, a new damage index is computed using natural frequencies and implementing a GMM to classify the bolted connection's state in a binary way. The advantage of the GMM is the ability to detect populations with different probability densities (Figueiredo et al., 2019). This approach is highly used for SHM assuming environmental variability. We can adapt it here to gather knowledge about torque fluctuation taking disassembly and assembly processes, generating considerable structural dynamics changes and, consequently, modal features associated with damage conditions.

The second method utilized is a stochastic interpolation obtained by GPR. The key idea is to learn the nonlinear correlation between the tightening torque and changes in the natural frequencies through the damage index previously computed based on them, assuming the uncertainties to validate these estimates' utilization. Although this correlation is empirical, as are several well-known phenomenological models in the literature (Mathis et al., 2020, Visintin, 2013), it is plausible to associate it with a reduced-order model that emulates the bolted joint's behavior. This is executed here to prove the GPR-based model's validity. Thus, we examine an equivalent reduced-order model of our experimental setup around the vibration mode that stresses the lap-joint the most to project the nonlinear restoring forces on a physical basis. Analyzing the restoring force \times displacement plane, it is worth noting that when there exists a decrease in the torque values applied to the contact patches of the Orion beam, the hysteresis loop becomes prominent and indicates the existence of a nonlinear relationship between the tightening torque and the natural frequencies. This effect is consistent with recent findings in the literature (Fantetti et al., 2019) since the tightening torque directly influences the normal load applied on the joint area. A higher torque value reduces the amount of slipping, resulting in a stiffer system.

Although reduced-order are usually capable of describing hysteresis effects and their influence on modal parameters, obtaining these models is difficult to achieve quickly, seeking to implement a practical SHM method. Thus, the proposal of a probabilistic methodology for tightening torque detection through simple features extracted from the modal parameters is justified. In addition to the introduction, this paper is organized as follows. In the first section, we present the problem statement, which addresses this work's main assumptions. Afterward, the methodology for detecting and quantifying the tightening torque is covered in the GMM and GPR sections, respectively. The Results and Discussion section starts with a description of the Orion beam used to demonstrate the method. Modal parameters are extracted directly from the frequency responses curves considering different torque levels. To validate the algorithm's effectiveness in detecting and estimating tightening torques under conditions involving variability in experimental realizations, frequency responses are measured considering three sets of complete assembly

and disassembly of the Orion beam. Finally, the concluding remarks summarize that applying the GMM helps detect early torque loss compared to the detection obtained with other methods. Moreover, the GPR enables us to learn the change score of the GMM. The proposed algorithm paves the way for its plausible application to different configurations of bolted structures.

Problem Statement and Methodology Framework

Some main questions are addressed to understand the problem correctly behind the experimental application under analysis:

- Problem tackled:
 - The Orion beam is used for proof-of-concept of the integrated approach proposed in this work. The academic test structure is representative of vibration effects common to systems assembled by bolted joints. The damage imposed on the structure aims to emulate a gradual loss of torque.
 - The system response exhibits random variations and a high degree of unrepeatability between measurements after complete assembly and disassembly of the lap-joint.
 - Nonlinearities may appear in the system's dynamic behavior for torque values referring to damage conditions.
 - The proposed approach needs to differentiate the influences from uncertainties, nonlinear behavior, and torque loss.

The key steps of the methodology used for tightening torque detection in bolted joints, which is based on using the GMM for damage detection and the GPR for quantification of the torque level, are described as follow:

- A set of vibration data in a healthy situation, i.e., a safe tightening torque, is known for different beam assemblies. Some features can be extracted from this data set. Here some sensitive natural frequencies are used as features to compute the damage index. Any traditional output-only modal analysis procedure can be applied to perform it.
- Using the learning data set in healthy condition, the GMM procedure is used to organize the probability distributions of the healthy state clusters and define a threshold value.
- Structural condition detection, i.e., determining whether the structure is damaged or not, is performed assuming different blind tests with unknown torques conditions (unknown health state). Damage indexes are then estimated.
- The relation between the damage index computed with the modal feature and the tightening torque level seems

to be nonlinear. Torque changes may cause variation in the energy dissipation when the tightening force applied to the bolts is reduced. This nonlinear relation is learned using a GPR with half of the damage index's available data set versus the tightening torque.

- The tightening torque quantification is performed by using the GPR-based model, which enables us to determine the mean and variance and infer our torque uncertainty estimates using a simple damage index. Blind tests are then considered to perform torque estimation with the calibrated GPR model.

Gaussian Mixture Model for Damage Detection

A Gaussian mixture model (GMM) is a practical machine learning algorithm for clustering using outlier formation. The components of a GMM are defined using a learning process to estimate the main clusters in the undamaged condition.

One may examine a learning data matrix, $\mathcal{Y} \in \mathbb{R}^{n \times d}$, with d -dimensional feature vectors from n different operational and environmental conditions when the structure is undamaged and a testing data matrix, $\mathcal{Z} \in \mathbb{R}^{l \times d}$, where l is the number of feature vectors from the undamaged or damaged conditions. Here the operational situation is the torque in the bolted joint assumed in the safe case (undamaged). Figure 1 shows the typical steps to implement a GMM for damage detection. First, learning using features is computed to define the central clusters by adjusting the features from \mathcal{Y} . Next, in the validation step, each new input feature vector from \mathcal{Z} is transformed in a damage index \mathcal{DI} , where it is feasible to observe a computed score to give the current state of a sample.

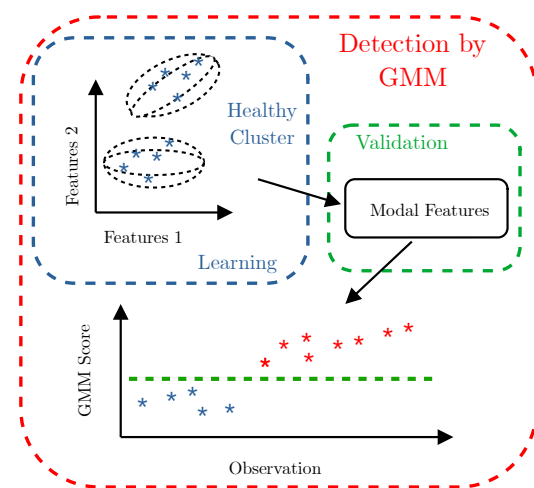


Figure 1. Algorithm for damage detection via Gaussian Mixture Model

A finite mixture model, $p(\mathbf{y}|\Theta)$, is the weighted sum of $K > 1$ components, $p(\mathbf{y}|\theta_k)$, in \mathbb{R}^d (McLachlan and Rathnayake, 2014)

$$p(\mathbf{y}|\Theta) = \sum_{k=1}^K \alpha_k p(\mathbf{y}|\theta_k), \quad (1)$$

where \mathbf{y} is the d -dimensional data vector and α_k corresponds to the weight of each component. These weights are constrained as $\alpha_k > 0$ with $\sum_{k=1}^K \alpha_k = 1$.

Each component $p(\mathbf{y}|\theta_k)$, is described by a Gaussian distribution

$$p(\mathbf{y}|\theta_k) = \frac{\exp\left[-\frac{1}{2}(\mathbf{y} - \boldsymbol{\mu}_k)^T \boldsymbol{\Sigma}_k^{-1}(\mathbf{y} - \boldsymbol{\mu}_k)\right]}{(2\pi)^{d/2} \sqrt{\det(\boldsymbol{\Sigma}_k)}}, \quad (2)$$

where each element denoted by the parameters, $\theta_k = \{\boldsymbol{\mu}_k, \boldsymbol{\Sigma}_k\}$, composed of the mean vector, $\boldsymbol{\mu}_k$, and the kernel matrix, $\boldsymbol{\Sigma}_k$. The parameters $\Theta = \{\alpha_1, \alpha_2, \dots, \alpha_K, \theta_1, \theta_2, \dots, \theta_K\}$ control entirely a GMM.

The expectation-maximization (EM) algorithm is the most used way to determine the parameters of the GMMs (Ganjavi et al., 2017). This strategy applies a maximization step until the log-likelihood, $\log p(\mathbf{Y}|\Theta) = \log \prod_{i=1}^m p(\mathbf{y}_i|\Theta)$, converges to a local optimum (McLachlan and Rathnayake, 2014). The Bayesian information criterion (BIC) can also be applied to define the appropriate number of structural elements for the fittest model of a GMM.

For each principal component k , a damage index is computed using each observation \mathbf{z} in the test matrix \mathcal{Z} :

$$\mathcal{DI}_k(\mathbf{z}) = (\mathbf{z} - \boldsymbol{\mu}_k) \boldsymbol{\Sigma}_k^{-1} (\mathbf{z} - \boldsymbol{\mu}_k)^T. \quad (3)$$

For each component, k , from the healthy situation, if a new observation, \mathbf{z} , is computed from the same element, \mathcal{DI}_k will be Chi-square distributed with d degrees of freedom, χ_d^2 . For each observation, the \mathcal{DI} is given by the smallest \mathcal{DI}_k estimated for each component

$$\mathcal{DI}(\mathbf{z}) = \min[\mathcal{DI}_1(\mathbf{z}), \dots, \mathcal{DI}_K(\mathbf{z})]. \quad (4)$$

Then, from a threshold established using the learning data, one can compare the data point to determine the structural state, in our case, the bolted joint's safety. The practical implementation can be performed using ready-made packages available, as Python (scikit-learn*).

Gaussian Process Regression for Tightening Torque Quantification

A Gaussian Process Regression (GPR) is a proper procedure for torque quantification to compute a learning model capable of associating the change in features with the tightening torque variation using a calibration procedure. It should be emphasized that these features can be damage indexes or a data set of modal parameters estimated for the learning and validation phases. However, since this work proposes an algorithm that integrates the detection and quantification methodologies, we chose to train the GPR based on the damage index.

The key idea is to estimate parameters for controlling a GPR model to infer the regression's variance and mean within a Bayesian paradigm, assuming that only limited information is available. The confidence interval tells us how much we can expect the model to detect changes in tightening torque or how risky it is to use it for this purpose. Figure 2 depicts the proposed algorithm to estimate the GPR-based model to quantify the torque state.

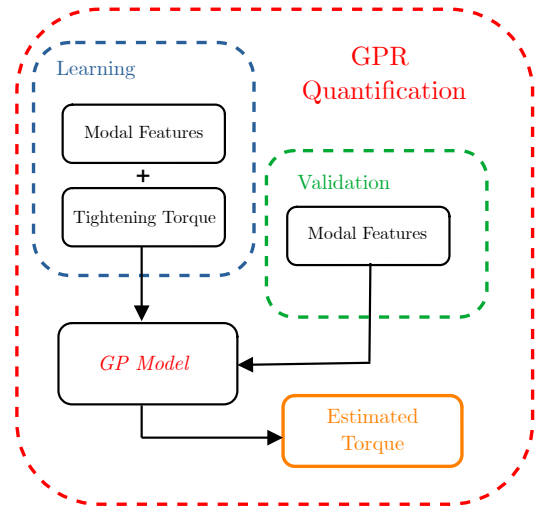


Figure 2. Algorithm for quantification of the tightening torque through the GP-based model.

The tightening torque $\mathcal{T}^{(i)} \in \mathbb{R}$ can be described as an output of a nonlinear regression (Rasmussen and Williams, 2006):

$$\mathcal{T}^{(i)} = f(\mathcal{F}^{(i)}) + \varepsilon_S^{(i)}, \quad i = 1, 2, \dots, N \text{ samples} \quad (5)$$

where $f(\cdot)$ is a nonlinear function, $\mathcal{F}^{(i)} \in \mathbb{R}$ is an input vector, in our case the damage index assumed known in the learning data, and $\varepsilon_S^{(i)}$ is a stochastic variable representing inherent randomness in the observations, which assumes a Gaussian distribution with zero mean:

*<https://scikit-learn.org/>

$$\varepsilon_S^{(i)} \sim \mathcal{N}(\varepsilon_S^{(i)} | 0, \sigma_S^2), \quad (6)$$

where σ_S^2 is the variance of the Gaussian noise observations. For N tests, the learning data set assumes the following simplified notation:

$$\mathcal{D} = \left(\mathcal{T}^{(i)}, \mathcal{F}^{(i)} \right)_{i=1}^N \equiv (\mathcal{T}, \mathcal{X}), \quad (7)$$

where $\mathcal{T} \in \mathbb{R}^{N \times 1}$ is the output vector (torques) and $\mathcal{X} \in \mathbb{R}^{N \times 1}$ is the input one (damage index).

Once the regression equation (5) represents a Gaussian Process, the function $f(\cdot)$ is then formed by the assumption of a multivariate Gaussian prior distribution of zero mean (Rasmussen and Williams, 2006):

$$\mathbf{f} = f(\mathcal{X}) \sim \mathcal{N}(\mathbf{f} | 0, \mathcal{K}), \quad (8)$$

where $\mathcal{K} \in \mathbb{R}^{N \times N}$ is the covariance (kernel) matrix with $\mathcal{K}_{ij} = k(\mathbf{x}_i, \mathbf{x}_j)$, and $k(\cdot, \cdot)$ is the *kernel* function, also named as covariance function (Paixão et al., 2021, Teloli et al., 2021b). The kernel function can assume several classes depending on the type of application. This function represent a degree of the agreement between two sample observations. In this work, considering the available data, the best results were achieved considering a squared exponential kernel as covariance function:

$$k(\mathbf{x}_i, \mathbf{x}_j) = \sigma^2 \exp \left[-\frac{1}{2} \left(\frac{x_i - x_j}{\ell} \right)^2 \right], \quad (9)$$

where σ^2 is the hyperparameter that controls the model's covariance and ℓ is the lengthscale. The hyperparameters $\beta = [\sigma^2, \ell]$ are determined by solving an optimization problem of the marginal log-likelihood of the observed data (Mattos et al., 2016):

$$\begin{aligned} \log p(\mathcal{T} | \mathcal{X}, \beta) &= -\frac{1}{2} \log |\mathcal{K} + \sigma_S^2 \mathcal{I}| + \\ &- \frac{1}{2} \mathcal{T}^T (\mathcal{K} + \sigma_S^2 \mathcal{I})^{-1} \mathcal{T} - \frac{N}{2} \log(2\pi), \end{aligned} \quad (10)$$

where $\mathcal{I} \in \mathbb{R}^{N \times N}$ is the identity matrix. In this work, such a maximization procedure is performed using an evolutionary optimization method, and the optimum model is used to predict new outputs as a result of new inputs.

The Bayesian inference is used to condition a posterior predictive distribution $p(\mathbf{f}_* | \mathcal{T}, \mathcal{X}, \mathbf{x}_*)$ over the predicted function \mathbf{f}_* based on the new input samples \mathbf{x}_* , which yields the main relationship for the GP regression (Rasmussen and Williams, 2006):

$$p(\mathbf{f}_* | \mathbf{x}_*, \mathcal{X}, \mathcal{T}) = \mathcal{N}(\mathbf{f}_* | \mu_*, \sigma_*^2), \quad (11)$$

where the posterior predictive mean is given by:

$$\mu_* = \mathbf{k}_{*N} (\mathcal{K} + \sigma_S^2 \mathcal{I})^{-1} \mathcal{T}, \quad (12)$$

and the posterior predictive variance is given by:

$$\sigma_*^2 = k_{**} - \mathbf{k}_{*N} (\mathcal{K} + \sigma_S^2 \mathcal{I})^{-1} \mathbf{k}_{N*}, \quad (13)$$

where

$$\begin{aligned} \mathbf{k}_{*N} &= [k(\mathbf{x}_*, \mathbf{x}_1), \dots, k(\mathbf{x}_*, \mathbf{x}_N)], \\ \mathbf{k}_{N*} &= \mathbf{k}_{*N}^T, \\ k_{**} &= k(\mathbf{x}_*, \mathbf{x}_*). \end{aligned}$$

A predictive distribution of \mathcal{T} is similar to f_* . The numerical implementation can be made using ready-made packages as available, for instance, in Matlab (UQLab[†], see Lataniotis et al. (2018)) or Python.

Results and Discussion

Description of the experimental setup

Figure 3 presents the experimental setup. The lap-joint structure, so-called ‘‘Orion beam’’ (Teloli et al., 2021), consists of two assembly duraluminium beams with dimensions of $200 \times 30 \times 2$ [mm] each one and connected by three M4 bolts spaced along a length of 30 mm, as depicted in Fig. 3. The beam is in a cantilever configuration under base excitation. To minimize uncertainties related to the stiffness in the cantilever beam's clamped boundary condition and avoid exciting torsional modes, a 40 mm length of the beam with the contact patches is screwed to a solid aluminum block, which is the base of the structure (see Fig. 3(c)).

The base motion is driven by a permanent magnetic shaker TIRA (TV Model 50303 – 120), which excites the structure considering a white-noise Gaussian input at an amplitude level of 4 m/s² RMS as the base acceleration. A Polytec vibrometer OFV-5000 is used to measure the velocity at the Orion beam's free end. In contrast, the acceleration at the base is monitored by a triaxial accelerometer PCB (Model 356A4). Base acceleration and velocity measurements are used to estimate the transmissibility spectrum. The setup also includes a National Instruments acquisition system composed of a CompactDAQ Chassis (NI cDAQ - 9134), C-Series Sound, and Vibration Input Module (NI-9263), and C-Series Voltage Output Module (NI-9234).

Concerning the bolted joint, there are contact patches at each bolt connection to retain the contact between both beams in a small area. These patches consist of a square

[†]<https://www.uqlab.com/>

of $12 \times 12 \text{ mm}^2$ with an extra thickness of 1 mm. After each experimental run, each bolt's torque value was checked by a Lindstrom MA500-1 torque wrench. Additionally, to avoid undesired uncertainties in the measured data set, the following assembly protocol was adopted for all experimental realizations:

1. To guarantee the alignment between both beams, two-axis are inserted in the external holes.
2. The central bolt is fully tightened.
3. Both axes are removed and the external bolts are thus tightened.

The damage imposed on the structure aims to emulate the gradual loss of torque. Preliminary tests indicate that variations in the preload values applied to the central bolt considerably alter the assembly's structural stiffness. Thus, to avoid abrupt changes in the system dynamics and ensure that the features' variation is gradual, the central bolt is maintained fully tightened with a torque of 80 cNm at all experimental measurements. On the other hand, 16 different levels of torque are considered ranging from 80 cNm to 5 cNm with decrement of 5 cNm. The torque range between 80 cNm to 60 cNm is assumed to be a safe/healthy condition, whereas from 55 cNm to 5 cNm, are taken as damaged conditions by loss of connecting properties.

One of the advantages of assembled structures over monolithic structures is that they can be assembled and disassembled according to operational needs. Unfortunately, these structures have high measurement-to-measurement variability (low repeatability between tests). This characteristic is because structural stiffness and damping properties are sensitive to changes in the contact area, influenced by several aspects, including contact pressure, residual stresses, roughness, surface alignment, dynamic clearance, friction, wear, and third body (see Brake et al. (2019), Jalali et al. (2019), for instance). Thus, to verify how robust our detection methodology is to the presence of variability in the lap-joint dynamics, experimental campaigns are performed on four sets of 15 measurements after complete assembly and disassembly of the Orion beam, repeated on different days to obtain a total of 60 realizations for each torque level.

Modal analysis

Figure 4(a) presents the transmissibility spectrum between the velocity measured at the free end of the beam (output) and the base acceleration (input) for some tightening torque conditions and different assemblies of the same beam. It can be seen that the bending modes of the beam are uncoupled and with reduced contribution from the torsional ones.

Figure 4(b) illustrates the modes predicted experimentally considering 195 sensing points on the Orion beam's surface. Note that lower modes have only a slight sensitivity to both changes in torque values and different assembly and disassembly realizations of the structure, as shown in Fig.

4(a) around 10 and 400 Hz. In contrast, the higher bending modes (approximately 700 and 1900 Hz) stress the lap-joint area more distinctly, ensuring greater observability of the effects of variations in resonance peaks.

Although it is known that bolted structures have inherent nonlinear behavior due to hysteresis effects induced by local frictional interactions at the joint, which indicates that a nonlinear identification might be more suitable on this class of issue (Teloli et al., 2021a), this paper adopts a more straightforward, but still traditional approach based on a classical modal analysis algorithm to extract the modal parameters; the so-called Complex Exponential Method (Maia and Silva, 2001). The key idea is to show that after a learning procedure involving combined linear parameters in different torque conditions, it is possible to associate them with the loosening in the bolted connection through a damage index.

Damping ratios are directly related to the quantification of nonlinear dissipation in friction-damped systems, including lap-joints (Festjens et al., 2013, Zare and Allen, 2021). It is expected that lower preload values, where the structure is less stiff, will maximize damping due to micro-slip motion. However, the damping ratios' estimation is more sensitive to noise than the natural frequencies (Cao et al., 2017), and for this reason, this paper considers only these frequencies as damage features.

To illustrate the sensibility of the natural frequencies to damage, Fig. 5 presents the boxplot of them for the first six bending modes for only one assembly. Note that in the 5th (Fig. 5(e)) and 6th (Fig. 5(f)) the resonance frequencies show a clear trend of decreasing values when the torque value is reduced. This trend in behavior is not seen in modes 1st, 2nd and 3rd (Figs. 5(a)-(c)). The 4th vibrating mode is also a feature candidate, with a trend comparable to modes 5th and 6th. However, preliminary tests indicated that including it in the feature space for learning would not significantly improve the algorithm's performance. Thus, the analysis follows with emphasis on modes 5th and 6th.

Figure 6 shows the natural frequencies of the 5th and 6th bending modes, including observations of the 960 tests performed for the 16 torque levels with 60 measurements for each of them and equally divided into four different assemblies. Each torque condition presents various tests that include variability in the feature maps (healthy and damaged conditions). The tightening torque is assumed the same in each realization by measurements with a torque wrench.

Challenges for damage detection in bolted joints by using modal parameters

Figure 7 illustrates potential pitfalls in classifying torque states for different assemblies by just individually interrogating natural frequencies as damage indexes since the mean and variance values in each condition are overlapping for most torque values (when assumed as a known label to

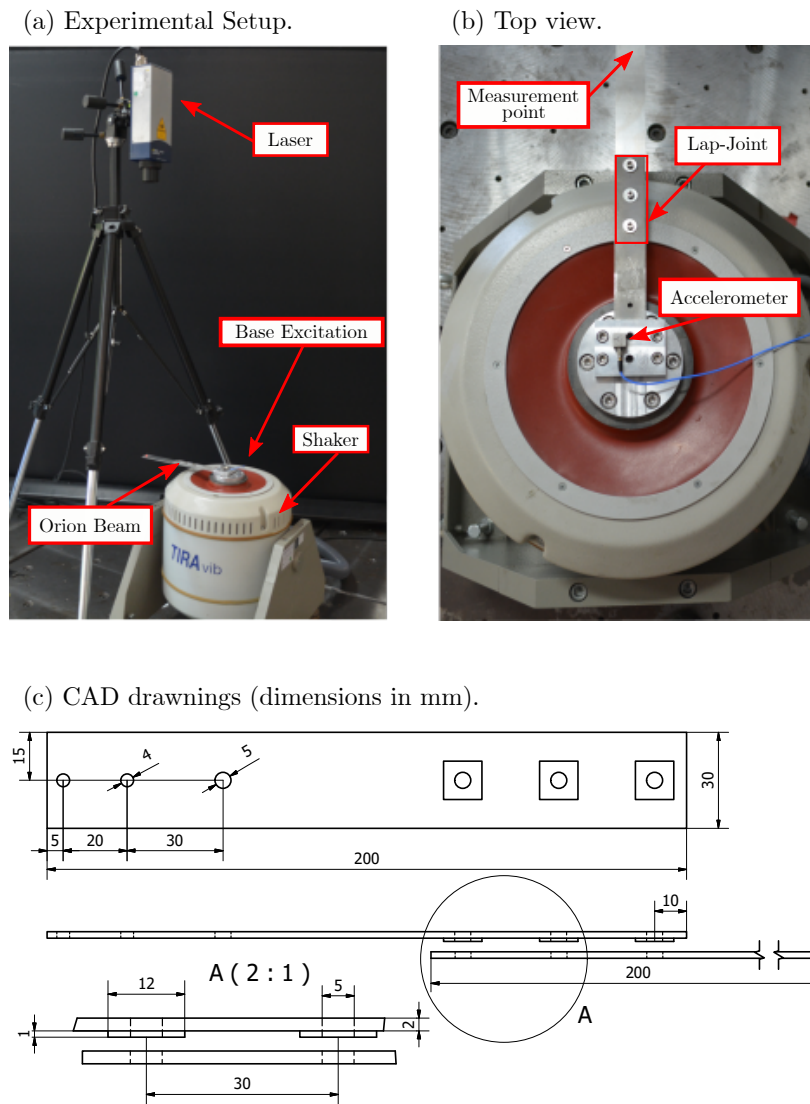


Figure 3. Experimental setup - The Orion beam (Teloli et al., 2021).

compare situations). Generally speaking, it is difficult to distinguish whether the changes are produced by damage, i.e., torque loosening or variability caused by fluctuating operational or environmental influences.

However, important information is hidden in the vibration data to explain what happens when the tightening torque decreases. The frictional contact produced between surfaces of bolted joints varies the damping properties. It results in the appearance of hysteresis loops, which can be seen through the plot of the restoring force from Fig. 8. The linear stiffness is driving the restoring force behavior at healthy torque conditions (80 and 60 cNm). Still, under damaged conditions, the hysteresis loop becomes more pronounced as the torque values decrease, as illustrated in Fig. 8. Here, the restoring forces, which represent the whole nonlinear force that actuates on the 6th vibrating mode (the bending modes are uncoupled and allow such approach), are identified by approximating an equivalent reduced-order model based on the force-state mapping (Jalali et al., 2007, Noel et al., 2012).

The dissipated energy caused by the hysteresis effect (such as the damping ratio) should also be a great feature as damage index; unfortunately, this parameter is difficult to estimate and identify as it generally requires an *a priori* updated reduced-order model. In this sense, it is preferable and straightforward to use a simple modal parameter, such as the natural frequency, as a feature.

The hysteresis' adequate slope slightly changes for low torque values, which indicates that the joint friction causes global stiffness nonlinearity. This effect occurs in jointed structures due to partial slippage on the joint interface, which reduces the contact stiffness according to the bolt preload applied (Brake et al., 2019, Jalali et al., 2019, Segalman, 2006). As a consequence, the natural frequency of the system is also sensitive to these variations in torque. Thus, the particular idea is to consider the natural frequencies that correspond to the 5th and 6th vibration modes to compute an index to classify the healthy or damaged states. Having covered the main challenges related to the torque detection in structures assembled by bolted joints, the following sections

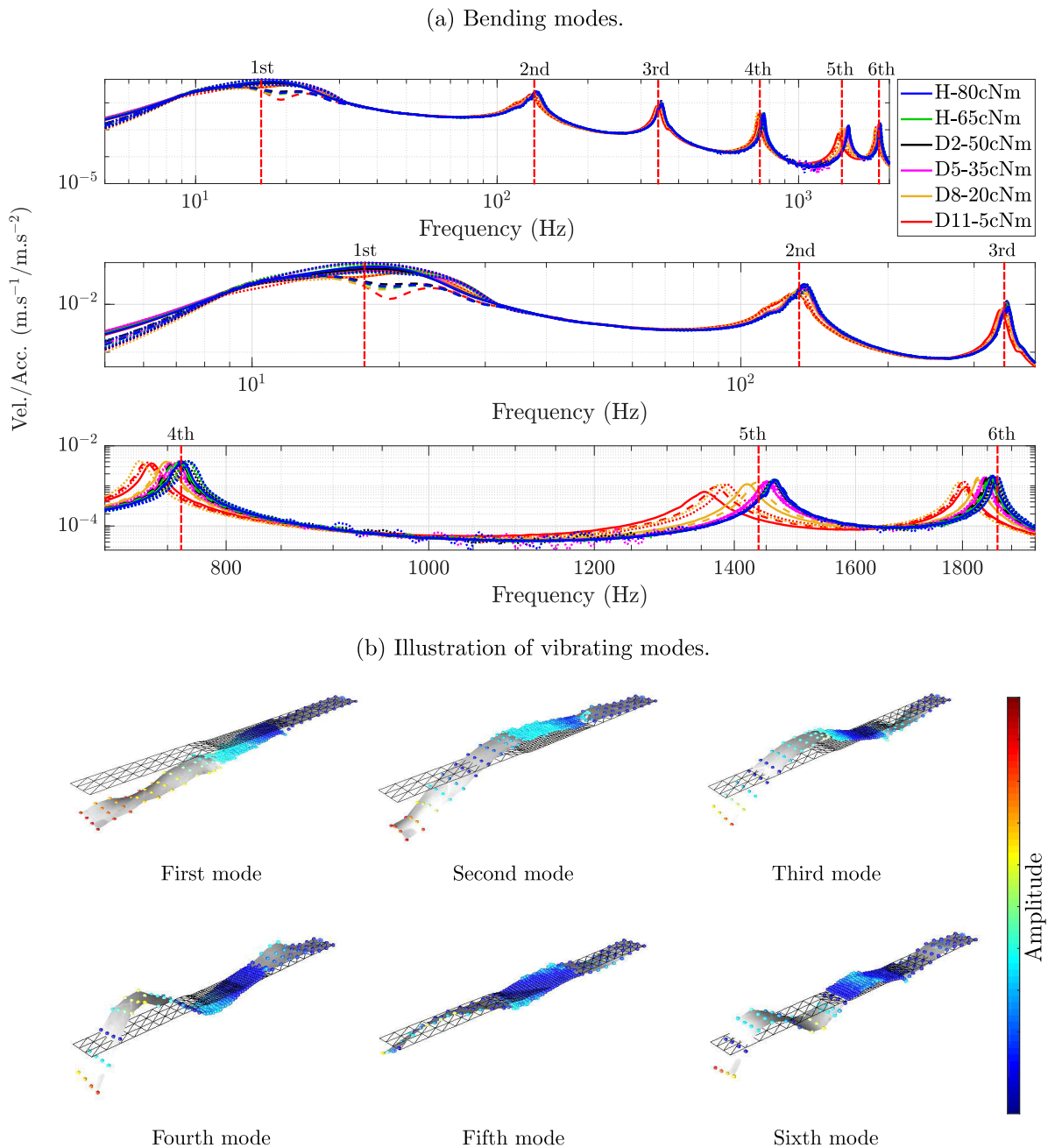


Figure 4. (a) Transmissibility plot with emphasis on the structural conditions. Dashed lines $--$ indicate the frequency ranges in which the bending modes are. Different lines of the same color indicates different assemblies; (b) exemplifies the experimentally measured modes.

aim to illustrate the methodology proposed by this work applied to experimental measurements.

Detecting torque loss by GMM

Classical classifiers that allocate the undamaged conditions into a single cluster, i.e., an overfitted probabilistic distribution, are unfeasible for classifying states from features of several torque conditions considering the assembly and disassembly procedure. In such types of classifiers, the DI s are calculated, for instance, by using the Mahalanobis Square Distance (MSD) between the learning data obtained from the features to a baseline

condition in a healthy state and the validation data under supposedly unknown torque conditions. However, since the characteristics of different assemblies may be distant from each other in their mapping (see the dispersion of the healthy state in Fig. 5), it is not feasible to classify test samples within a cluster that has a higher concentration of observations far from the mean of its distribution as healthy without any baseline data indicating healthy condition near to this unrepresentative mean, as could occur when considering an algorithm based on a single distribution for all the undamaged data, i.e., $K = 1$ cluster. In this case, there is the possibility of overlap between the reference state and a damaged one (see Fig. 5), indicating as healthy conditions those situations where damage exists (in particular to this

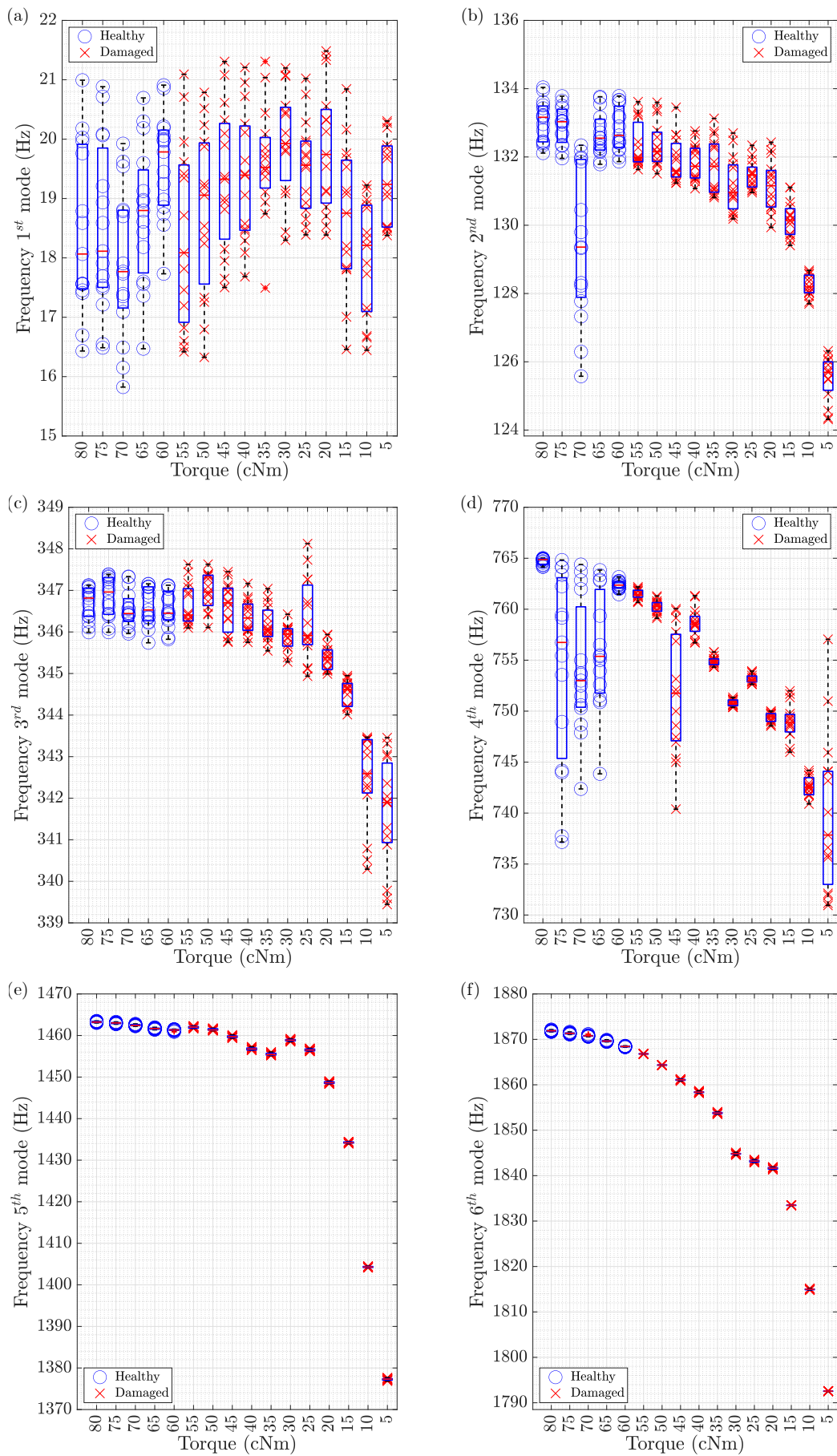


Figure 5. Boxplot of the resonance frequencies referring to the 1st (a), 2nd (b), 3rd (c), 4th (d), 5th (e) and 6th (f) bending modes on different tightening torques in each labeled structural condition.

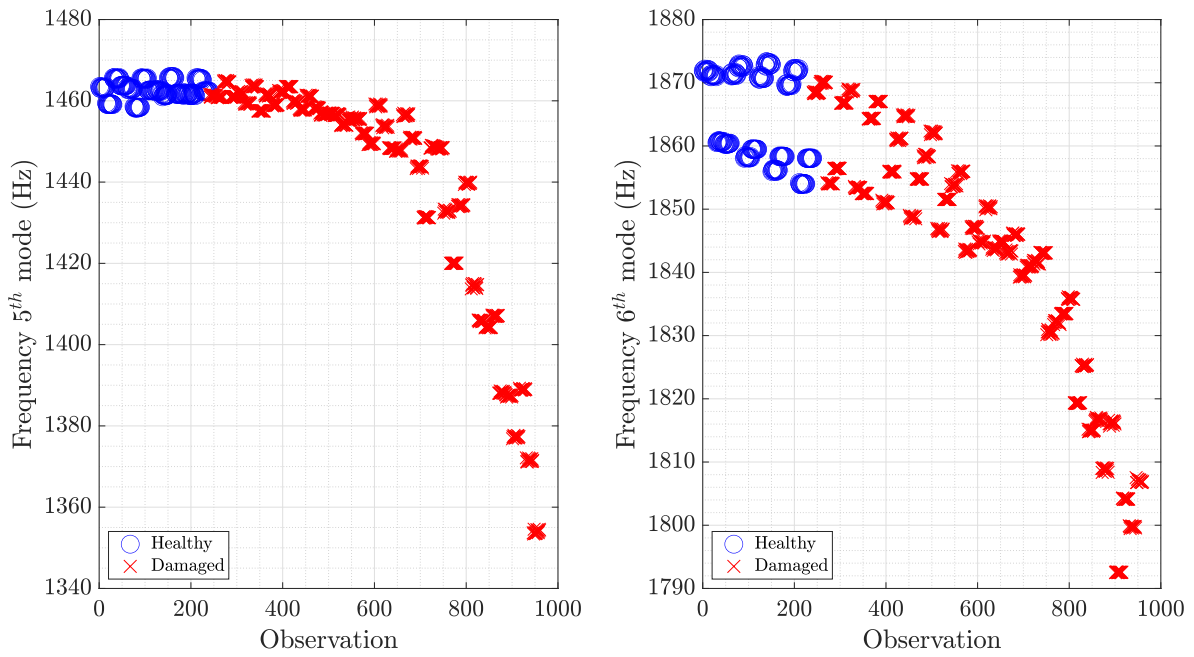


Figure 6. Experimental identification, changing the **tightening torque** with 180 observations (36 in each structural conditions equally distributed in three different assemblies) to show the **variability** of the natural frequencies

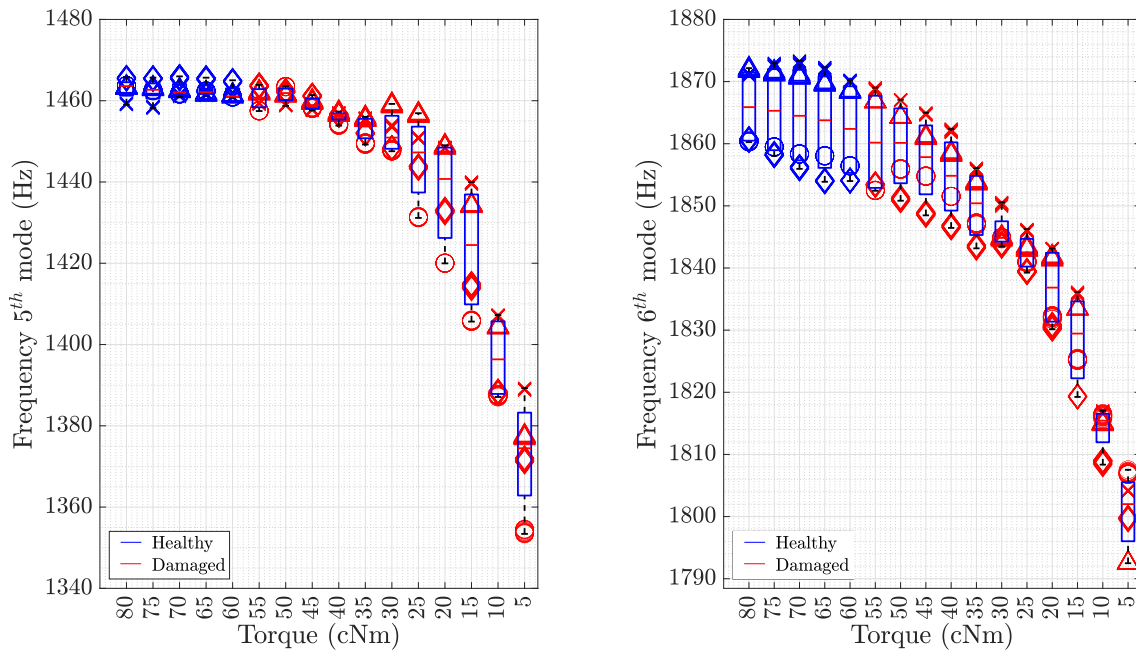


Figure 7. Boxplot of the resonance frequencies on different tightening torques using three realizations in each **labeled structural condition** and **different set of assemblies** indicated by markers: \triangle , \times and \diamond .

work, **most tests between 55 and 45 cNm would be incorrectly classified as healthy**), presenting high values of type II errors. For this reason, GMM is used in this work to form $K > 1$ cluster components referring to the baseline conditions (undamaged states).

For the GMM learning, half of the data set referring to safe torque conditions (**from 80 to 60 cNm**) is randomly selected within the sample space of features **for each assembly**. The remaining **healthy data** are used to validate **false-positive** errors and observe the clustering performance of the

GMM-based algorithm. Table 1 summarizes how the feature samples are used in this work.

For the GMM learning procedure, a number of $K = 9$ components are used to represent the data in the healthy state. This number is chosen based on the Bayesian information criterion (BIC). The clearest way to understand how the GMM algorithm deals with the data set to classify the structural states as healthy or not is by visualizing the learned model and dispersing the features' clusters. Figure 9 illustrates the multivariate probability density functions

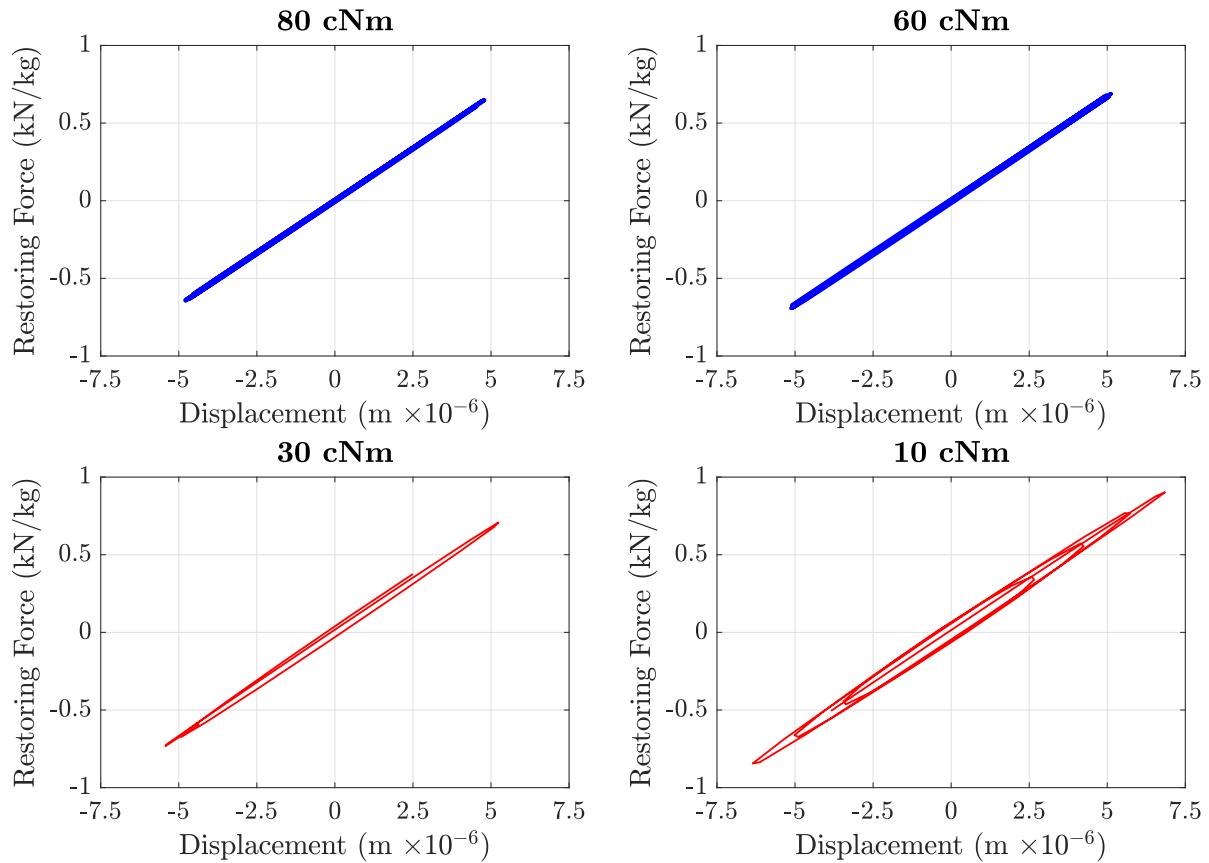


Figure 8. Restoring forces that actuate on the 6th bending mode projected on physical basis; hysteresis loop opening when the tightening torque reduces, modifying the natural frequencies in a nonlinear way.

Table 1. Parameters for learning and validation.

Data Set	Condition	Number of Samples	Range of torque (cNm)
learning	Healthy	150	80, 75, 70, 65, 60
Validation	Healthy	150	80, 75, 70, 65, 60
Validation	Damaged	660	55, 50, 45, 40, 35, 30, 25, 20, 15, 10, 5

(PDF) learned by the GMM. The clusters also demonstrate the possible effectiveness of the model in detecting outliers for damage classification. This can be seen because all test data in healthy conditions are concentrated at the learned PDFs, and those in damaged conditions are far away. The MSD is responsible for computing the damage indexes based on the nearest healthy cluster's outlier formation. **Note that some limitations to early detection may appear when a large number of assemblies to the GMM model is considered. Although the GMM prevents most false-positive occurrences by introducing multiple healthy clusters, it is still possible for a healthy cluster from an assembly to overlap a damaged condition from another one. In this case, the error in condition detection is difficult to avoid, as there would be no distinction between samples in feature space. However, this would generally occur for some cases of early detection (in this work, for 55 cNm and 50 cNm torque values).**

Figure 10 shows the classification results where the type I errors (false-positive) are $\approx 3.6\%$ and the type II errors (false-negative) are $\approx 0\%$ for all validation data, proving that the identified GMM can detect the changes caused by fluctuations in tightening torque values with good performance, and is suitable for use even in situations where different assembly sets are considered. To establish the threshold value, the Chi-square test was applied.

The results' analysis indicates that it was possible to recognize a reduction in the torque values from the 80 - 60 cNm conditions to 55 - 5 cNm based on the proposed *DL*. Compared to methods in the literature using modal parameters, just a considerable loss of tightening torque is detected with statistical confidence, as performed by Luo and Yu (2017), where only changes for tightening were observed from 20 Nm in the undamaged condition to 2.5 Nm in the damaged one. Furthermore, it is also important to stress that

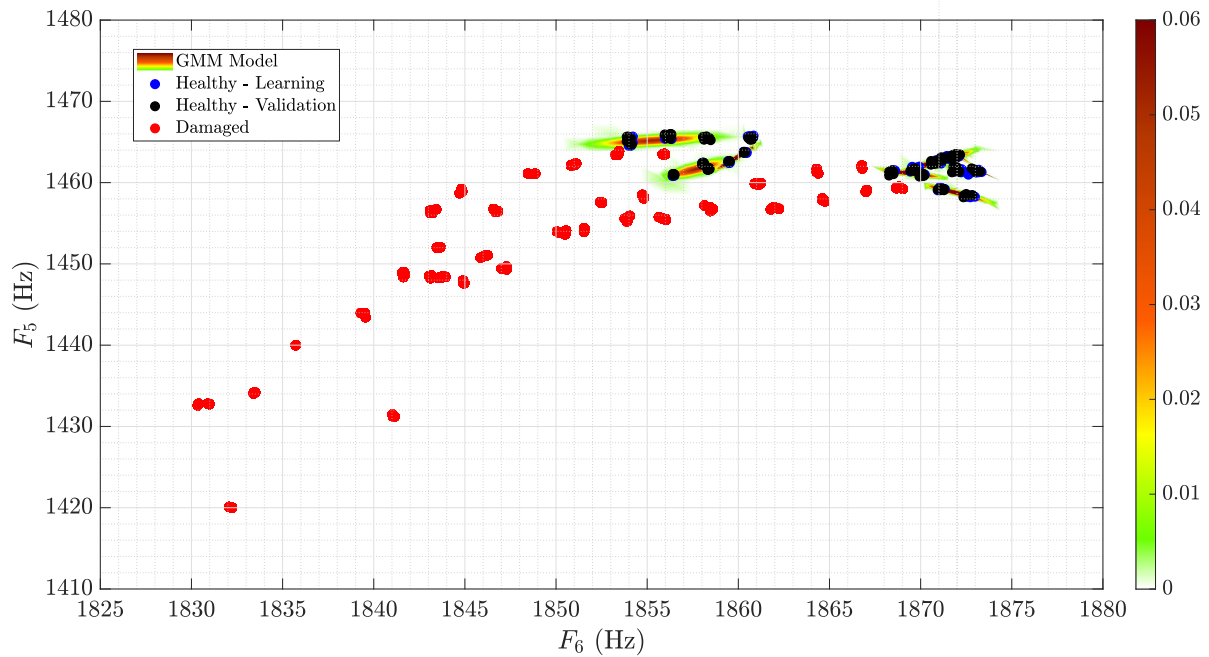


Figure 9. Learned GMM and features clustering.

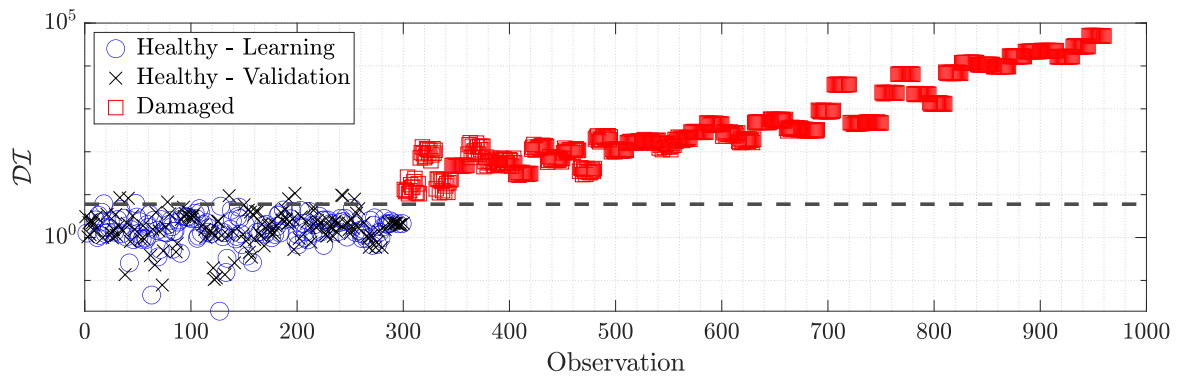


Figure 10. DI computed by GMM using frequencies of the 5th and 6th modes. Type I Error are $\approx 2.8\%$ and Type II Error are $\approx 0\%$.

the structure tested by these authors consisted of a single bolted joint, which is a setup quite sensitive to variations in the applied preload.

The following considerations and benefits in using the GMM are outlined:

- The advantage of applying GMM is to make several distributions of different assembly configurations to learn how the modal parameters change when the torque is changed, making it easier to detect outliers. However, attention must be paid. In practical terms, with each new structure assembly, new clusters associated with the healthy condition must be produced. This fact is not a direct limitation of the method, since the assembly protocol is expected to guarantee torque values consistent with the healthy condition;
- Another advantage is that the amount of samples used for learning is not exhaustive to measure;
- For this application where it is only intended to detect whether or not torque loss exists and not to locate the position of the damage, a single measurement point is satisfactory for extracting features based on the modal parameters;
- The approach is not limited to using only vibration signals and modal parameters; other time-series features could be used to extract additional damage-sensitive indicators to calculate the score for classification - for instance, the use of output-only methods is adequately acceptable to apply. Nonetheless, caution should be taken since some features extracted in output-only

methods capture global vibration effects, which may compromise the damage position's detection.

Tightening torque estimation via GPR

A natural and subsequent step to detecting the loss of tightening torque is to estimate this value without the need for a direct measurement using, for instance, a torque wrench or structural inspection *in locus*. Since natural frequency-based DI can track torque variations, this score is used to calibrate the GPR learning for torque estimation.

The learning data $(\mathcal{T}, \mathcal{X})$ used for learning the GPR-based model and estimation of hyperparameters β consist of half of the observed DI samples randomly selected within a uniform distribution to form the learning input vector \mathcal{X} , whereas the torque values corresponding to each DI are the output vector \mathcal{T} . The remaining DI samples are used for validation of the GPR-based model.

Figure 11 depicts the GPR-based model's predicted torque with 95% of statistical confidence bands in direct comparison with validation data. Note that the model has large confidence bands for low torque values, even covering negative torque values. The explanation for this refers to the dispersion of the features observed to compute the DI . Note in Fig. 5 that for the 5th resonance frequency, the variability between the different assemblies increases as the tightening torque decreases. This result is expected since the uncertainties related to contact pressure distribution are reduced when the preload increases. It is noteworthy that there is a tendency for more pronounced reductions in the natural frequency the lower the tightening torque. In this context, the MSD increases similarly to low torque values, making the points more distant from each other and thus hampering the regression in this region. It also stands out that the relationship between torque and DI s is not monotonic. This is because there are more than one DI with the same torque as well as more than one torque for the same DI . Nonetheless, this GPR-based model can help the user decide about tightening torque based on score changes and, consequently, quantify possible damages.

Figure 12 presents the comparison of the actual *versus* estimated torques. It is worth noting that the estimated mean values are close to each torque condition's actual ones, especially for damaged conditions. There are some expected limitations in accurately estimating the tightening torque in healthy conditions, as all of them are considered to be on the reference state when computing the MSD. Therefore the DI tends to be ≈ 0 in both. The zoom is shown in Fig. 11 reveals that for all conditions between 80 and 60 cNm, a mean torque of ≈ 70 cNm is predicted. Since both states are defined as indistinguishable healthy states, one can conclude that there is no loss in this particular imprecision.

Combining the GMM and GPR algorithms to first detect whether there is damage to the structural connection and subsequently, in an affirmative case, quantify the severity of the damage with reasonable accuracy is a simple tool

with the potential to aid decision-making in maintenance procedures involving bolted joints. This result is feasible for industrial applications once a calibrated GPR-based model is obtained after a supervised learning procedure. Based on this, the most viable alternative is to consider the mean or even the upper and/or lower limits of confidence bands to make a safer decision.

Conclusions

This paper proposes a procedure for detecting tightening torque loss for structures assembled by bolted joints based on probabilistic machine learning tools. The motivation of this work arises from the need to interpret and differentiate which variations in the structural dynamics of bolted joints are related to changes in the preload applied to them (which is considered damage in this work), from variations arising from operational conditions and uncertainties inherent to these systems that are not necessarily damaged, such as the assembly and disassembly procedure.

It is argued that one of the advantages of this work lies in using modal parameters as features to compute damage indexes. The extraction of these parameters can be done by any traditional modal analysis procedure and does not require multi-point measurements to be observed by the acquisition system. In particular to this work, natural frequencies of two vibrating modes are chosen as features. In bolted joints, the variation in these parameters' values may be related to changes in the system's structural stiffness caused by alterations in tightening torque. Data variation was imposed on the experimental setup by considering vibration measurements after complete assembly and disassembly of the Orion beam.

Extracted features were used in the learning step of the Gaussian mixture model. The advantage of applying GMM is to make several distributions of different assembly configurations to understand how the modal parameters change when the torque is changed, which aids in recognizing outliers. To this end, damage indexes were computed by the Mahalanobis square distance. Consequently, with the GMM correctly identified to classify states into damaged or undamaged conditions, there was a low occurrence of type I errors (3.6%) and no type II errors. This procedure is suitable for implementing an automated alarm system for bolted joint application on flanges, pipes, or offshore structures, using indirect vibration measurements, i.e., without the need for sensors allocated to each bolt of the connection.

A GPR-based model's learning was carried out by using the estimated damage indexes for several torque conditions. In practical terms for the application addressed in this paper, one first classifies whether the damage is present (loss of tightening torque) and then estimates the actual torque condition. Due to the sparse amount of torque states for learning the GPR-based model, the healthy condition's assessed value will probably differ from the real torque

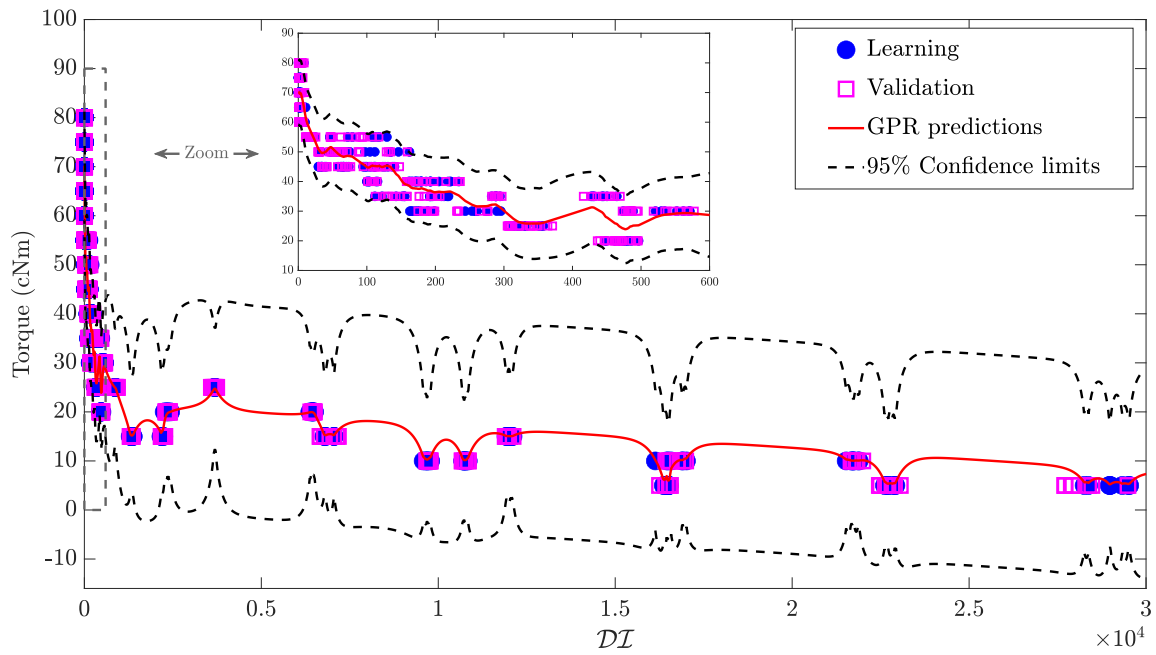


Figure 11. Torque versus DI with a GPR model.

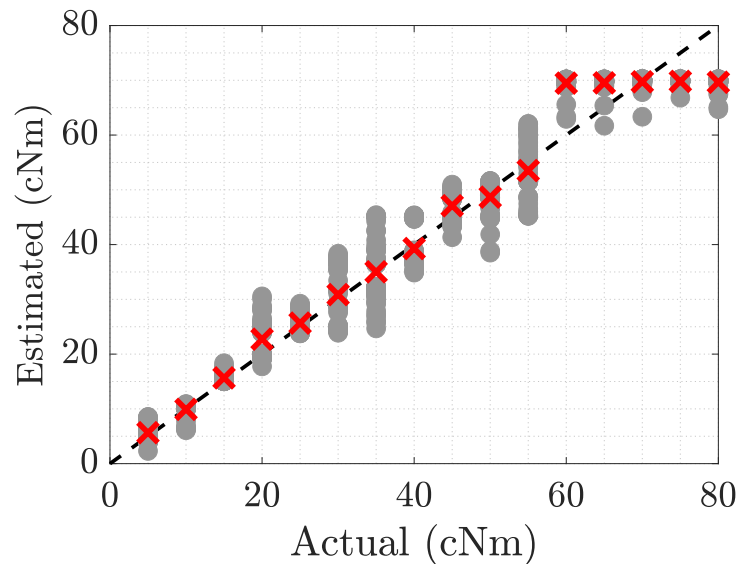


Figure 12. Estimated torque versus actual torque for all index (•) (gray) and the mean of estimated torque (×) (red) in each test condition.

value. However, when damage exists, it is possible to quantify its severity with reasonable accuracy. The results presented in this paper are concerned with explaining the probabilistic model learning via the GMM and GPR in the academic test structure. The natural path to be followed is to validate the methodology to detect tightening torque variations in large structures (e.g., offshore structures). To achieve this, additional experiments will be collected to test asymmetric variations of torque applied on the external bolts or even on the central bolt to ensure that the methodology is robust in an even more uncertain scenario close to industrial applications. In this context, this work paves the way to validate other features extracted directly from time-series or additional spectral information about the frequency responses. **Moreover, other future applications of industrial**

interest could be the use of the GMM approach to monitor more than one assembly of nominally identical structures acting simultaneously with just one classifier trained for all of them, which could simplify the damage detection for an entire population of specimens.

Declaration of conflicting interests

The authors declared no potential conflicts of interest concerning the research, authorship, and/or publication of this article.

Funding

The authors would like to thank the financial support provided by the Brazilian National Council for Scientific and Technological Development (CNPq) grant number 306526/2019-0, São Paulo Research Foundation (FAPESP) grant numbers 16/21973-5, 19/19684-3, and 20/07449-7; and Bourgogne Franche-Comté Region in collaboration with EUR EIPHI Graduate School contract ANR-17-EURE-0002.

References

- Brake M, Schwingshackl C and Reuß P (2019) Observations of variability and repeatability in jointed structures. *Mechanical Systems and Signal Processing* 129: 282 – 307. DOI:<https://doi.org/10.1016/j.ymsp.2019.04.020>. URL <http://www.sciencedirect.com/science/article/pii/S0888327019302511>.
- Brake MR (2018) *The Mechanics of Jointed Structures: Recent Research and Open Challenges for Developing Predictive Models for Structural Dynamics*. Springer. DOI:<https://doi.org/10.1007/978-3-319-56818-8>.
- Cao M, Sha G, Gao Y and Ostachowicz W (2017) Structural damage identification using damping: a compendium of uses and features. *Smart Materials and Structures* 26(4): 043001.
- Cha YJ, You K and Choi W (2016) Vision-based detection of loosened bolts using the hough transform and support vector machines. *Automation in Construction* 71: 181 – 188. DOI:<https://doi.org/10.1016/j.autcon.2016.06.008>. URL <http://www.sciencedirect.com/science/article/pii/S0926580516301297>.
- Chou JS, Ou YC, Lin KY and Wang ZJ (2018) Structural failure simulation of onshore wind turbines impacted by strong winds. *Engineering Structures* 162: 257–269. DOI:<https://doi.org/10.1016/j.engstruct.2018.02.006>. URL <https://www.sciencedirect.com/science/article/pii/S0141029617323945>.
- Doyle D, Zagrai A, Arritt B and Çakan H (2010) Damage detection in bolted space structures. *Journal of Intelligent Material Systems and Structures* 21(3): 251–264. DOI:[10.1177/1045389X09354785](https://doi.org/10.1177/1045389X09354785). URL <https://doi.org/10.1177/1045389X09354785>.
- Fantetti A, Tamatam L, Volvert M, Lawal I, Liu L, Salles L, Brake M, Schwingshackl C and Nowell D (2019) The impact of fretting wear on structural dynamics: Experiment and simulation. *Tribology International* 138: 111–124. DOI:<https://doi.org/10.1016/j.triboint.2019.05.023>. URL <https://www.sciencedirect.com/science/article/pii/S0301679X19302828>.
- Festjens H, Chevallier G and Dion JI (2013) A numerical tool for the design of assembled structures under dynamic loads. *International Journal of Mechanical Sciences* 75: 170–177. DOI:<https://doi.org/10.1016/j.ijmecsci.2013.06.013>. URL <https://www.sciencedirect.com/science/article/pii/S0020740313001860>.
- Figueiredo E, Moldovan I, Santos A, Campos P and Costa JCWA (2019) Finite element-based machine-learning approach to detect damage in bridges under operational and environmental variations. *Journal of Bridge Engineering* 24(7): 04019061. DOI:[https://www.doi.org/10.1061/\(ASCE\)BE.1943-5592.0001432](https://www.doi.org/10.1061/(ASCE)BE.1943-5592.0001432).
- Ganjavi A, Christopher E, Johnson CM and Clare J (2017) A study on probability of distribution loads based on expectation maximization algorithm. In: *2017 IEEE Power Energy Society Innovative Smart Grid Technologies Conference (ISGT)*. pp. 1–5. DOI:[10.1109/ISGT.2017.8086037](https://doi.org/10.1109/ISGT.2017.8086037).
- Jalali H, Ahmadian H and Mottershead JE (2007) Identification of nonlinear bolted lap-joint parameters by force-state mapping. *International Journal of Solids and Structures* 44(25): 8087–8105. DOI:<https://doi.org/10.1016/j.ijsolstr.2007.06.003>. URL <https://www.sciencedirect.com/science/article/pii/S0020768307002417>.
- Jalali H, Haddad Khodaparast H, Madinei H and Friswell M (2019) Stochastic modelling and updating of a joint contact interface. *Mechanical Systems and Signal Processing* 129: 645 – 658. DOI:<https://doi.org/10.1016/j.ymsp.2019.04.003>.
- Lataniotis C, Marelli S and Sudret B (2018) The Gaussian process modelling module in UQLab.
- Li Q and Jing X (2017) A second-order output spectrum approach for fault detection of bolt loosening in a satellite-like structure with a sensor chain. *Nonlinear Dynamics* 89(1): 587–606. DOI:[10.1007/s11071-017-3473-6](https://doi.org/10.1007/s11071-017-3473-6). URL <https://doi.org/10.1007/s11071-017-3473-6>.
- Li Q and Jing X (2020) Fault diagnosis of bolt loosening in structures with a novel second-order output spectrum-based method. *Structural Health Monitoring* 19(1): 123–141. DOI:[10.1177/1475921719836379](https://doi.org/10.1177/1475921719836379). URL <https://doi.org/10.1177/1475921719836379>.
- Luo WF and Yu L (2017) New damage-sensitive feature for structures with bolted joints. *Journal of Physics: Conference Series* 842: 012083. DOI:[10.1088/1742-6596/842/1/012083](https://doi.org/10.1088/1742-6596/842/1/012083). URL <https://doi.org/10.1088/1742-6596/842/1/012083>.
- Maia N and Silva J (2001) Modal analysis identification techniques. *Philosophical Transactions of the Royal Society of London. Series A: Mathematical, Physical and Engineering Sciences* 359(1778): 29–40.
- Mathis AT, Balaji NN, Kuether RJ, Brink AR, Brake MRW and Quinn DD (2020) A Review of Damping Models for Structures With Mechanical Joints. *Applied Mechanics Reviews* 72(4). DOI:[10.1115/1.4047707](https://doi.org/10.1115/1.4047707). URL <https://doi.org/10.1115/1.4047707>. 040802.
- Mattos CLC, Damianou A, Barreto GA and Lawrence ND (2016) Latent Autoregressive Gaussian Processes Models for Robust System Identification. *IFAC-PapersOnLine* 49(7): 1121 – 1126. DOI:<https://doi.org/10.1016/j.ifacol.2016.07.353>. URL <http://www.sciencedirect.com/science/article/pii/S2405896316305602>. 11th IFAC Symposium on Dynamics and Control of Process Systems Including Biosystems DYCOPS-CAB 2016.
- McLachlan GJ and Rathnayake S (2014) On the number of components in a Gaussian mixture model. *WIREs Data Mining and Knowledge Discovery* 4(5): 341–355. DOI:<https://doi.org/10.1002/widm.1135>. URL <https://onlinelibrary.wiley.com/doi/abs/10.1002/widm.1135>.
- Meyer JJ and Adams DE (2019) Using impact modulation to quantify nonlinearities associated with bolt loosening with applications to satellite structures. *Mechanical Systems and Signal Processing* 116: 787 – 795. DOI:<https://doi.org/10.1016/j.ymsp.2018.06.042>. URL <http://www.sciencedirect.com>.

- com/science/article/pii/S0888327018303819.
- Miao R, Zhang S and Xue S (2020) A review of bolt tightening force measurement and loosening detection. *Sensors* 20(1): 3165. URL <https://doi.org/10.3390/s20113165>.
- Milanese A, Marzocca P, Nichols J, Seaver M and Trickey S (2008) Modeling and detection of joint loosening using output-only broad-band vibration data. *Structural Health Monitoring* 7(4): 309–328. DOI:10.1177/1475921708090565. URL <https://doi.org/10.1177/1475921708090565>.
- Motosh N (1976) Development of design charts for bolts preloaded up to the plastic range. *Journal of Engineering for Industry* 98: 849–851.
- Nazarko P and Ziemianski L (2017) Force identification in bolts of flange connections for structural health monitoring and failure prevention. *Procedia Structural Integrity* 5: 460 – 467. DOI:<https://doi.org/10.1016/j.prostr.2017.07.142>. URL <http://www.sciencedirect.com/science/article/pii/S2452321617302548>. 2nd International Conference on Structural Integrity, ICSI 2017, 4-7 September 2017, Funchal, Madeira, Portugal.
- Nikravesh SMY and Goudarzi M (2017) A Review Paper on Looseness Detection Methods in Bolted Structures. *Latin American Journal of Solids and Structures* 14: 2153 – 2176. URL http://www.scielo.br/scielo.php?script=sci_arttext&pid=S1679-78252017001202153&nrm=iso.
- Noel JP, Kerschen G and Newerla A (2012) Application of the restoring force surface method to a real-life spacecraft structure. In: Adams D, Kerschen G and Carrella A (eds.) *Topics in Nonlinear Dynamics, Volume 3*. New York, NY: Springer New York. ISBN 978-1-4614-2416-1, pp. 1–19.
- Oregui M, Li S, Núñez A, Li Z, Carroll R and Dollevoet R (2017) Monitoring bolt tightness of rail joints using axle box acceleration measurements. *Structural Control and Health Monitoring* 24(2): e1848. DOI:<https://doi.org/10.1002/stc.1848>. URL <https://onlinelibrary.wiley.com/doi/abs/10.1002/stc.1848>. E1848 STC-14-0173.R3.
- Paixão J, da Silva S, Figueiredo E, Radu L and Park G (2021) Delamination area quantification in composite structures using Gaussian process regression and auto-regressive models. *Journal of Vibration and Control* 0(0): 1077546320966183. URL <https://doi.org/10.1177/1077546320966183>.
- Park G, Cudney HH and Inman DJ (2001) Feasibility of using impedance-based damage assessment for pipeline structures. *Earthquake Engineering & Structural Dynamics* 30(10): 1463–1474. DOI:<https://doi.org/10.1002/eqe.72>. URL <https://onlinelibrary.wiley.com/doi/abs/10.1002/eqe.72>.
- Qiu L, Yuan S, Chang FK, Bao Q and Mei H (2014) On-line updating gaussian mixture model for aircraft wing spar damage evaluation under time-varying boundary condition. *Smart Materials and Structures* 23(12): 125001. DOI:10.1088/0964-1726/23/12/125001. URL <https://doi.org/10.1088/0964-1726/23/12/125001>.
- Ramana L, Choi W and Cha YJ (2019) Fully automated vision-based loosened bolt detection using the Viola–Jones algorithm. *Structural Health Monitoring* 18(2): 422–434. DOI:10.1177/1475921718757459. URL <https://doi.org/10.1177/1475921718757459>.
- Rasmussen CE and Williams CKI (2006) *Gaussian Processes for Machine Learning*. Cambridge, MA, USA: Massachusetts Institute of Technology - MIT Press.
- Razi P, Esmaeel RA and Taheri F (2013) Improvement of a vibration-based damage detection approach for health monitoring of bolted flange joints in pipelines. *Structural Health Monitoring* 12(3): 207–224. DOI:10.1177/1475921713479641. URL <https://doi.org/10.1177/1475921713479641>.
- Reza M, Bursi O, Paolacci F and Kumar A (2014) Enhanced seismic performance of non-standard bolted flange joints for petrochemical piping systems. *Journal of Loss Prevention in the Process Industries* 30: 124–136. DOI:<https://doi.org/10.1016/j.jlp.2014.05.011>. URL <https://www.sciencedirect.com/science/article/pii/S0950423014000850>.
- Segalman DJ (2006) Modelling joint friction in structural dynamics. *Structural Control and Health Monitoring* 13(1): 430–453.
- Siewert C, Panning L, Wallaschek J and Richter C (2010) Multiharmonic Forced Response Analysis of a Turbine Blading Coupled by Nonlinear Contact Forces. *Journal of Engineering for Gas Turbines and Power* 132(8). DOI:10.1115/1.4000266. URL <https://doi.org/10.1115/1.4000266>. 082501.
- Teloli RO, Butaud P, Chevallier G and da Silva S (2021) Good practices for designing and experimental testing of dynamically excited jointed structures: the Orion beam. *Manuscript submitted for publication*.
- Teloli RO, da Silva S, Ritto TG and Chevallier G (2021a) Bayesian model identification of higher-order frequency response functions for structures assembled by bolted joints. *Mechanical Systems and Signal Processing* 151: 107333. DOI:<https://doi.org/10.1016/j.ymssp.2020.107333>. URL <https://www.sciencedirect.com/science/article/pii/S0888327020307196>.
- Teloli RO, Villani LG, da Silva S and Todd MD (2021b) On the use of the GP-NARX model for predicting hysteresis effects of bolted joint structures. *Mechanical Systems and Signal Processing* 159: 107751. DOI:<https://doi.org/10.1016/j.ymssp.2021.107751>. URL <https://www.sciencedirect.com/science/article/pii/S0888327021001461>.
- Villani LGG, da Silva S, Cunha A and Todd MD (2020) On the detection of a nonlinear damage in an uncertain nonlinear beam using stochastic Volterra series. *Structural Health Monitoring* 19(4): 1137–1150. DOI:10.1177/1475921719876086. URL <https://doi.org/10.1177/1475921719876086>.
- Visintin A (2013) *Differential models of hysteresis*, volume 111. Berlin: Springer Science & Business Media. URL <http://www.doi.org/10.1007/978-3-662-11557-2>.
- Wang F, Chen Z and Song G (2020) Monitoring of multi-bolt connection looseness using entropy-based active sensing and genetic algorithm-based least square support vector machine. *Mechanical Systems and Signal Processing* 136: 106507. DOI:<https://doi.org/10.1016/j.ymssp.2019.106507>. URL <http://www.sciencedirect.com/science/article/pii/S0888327019307289>.
- Wang F and Song G (2019) Bolt early looseness monitoring using modified vibro-acoustic modulation by time-reversal. *Mechanical Systems and Signal Processing* 130: 349 – 360. DOI:<https://doi.org/10.1016/j.ymssp.2019.04.036>. URL <http://www.sciencedirect.com/science/article/pii/S0888327019302730>.
- Wang T, Song G, Liu S, Li Y and Xiao H (2013a) Review of bolted connection monitoring. *International Journal of Distributed Sensor Networks* 9(12): 871213. DOI:10.1155/2013/871213. URL <https://doi.org/10.1155/2013/871213>.

- Wang T, Song G, Liu S, Li Y and Xiao H (2013b) Review of bolted connection monitoring. *International Journal of Distributed Sensor Networks* 9(12): 871213. DOI:10.1155/2013/871213. URL <https://doi.org/10.1155/2013/871213>.
- Zare I and Allen MS (2021) Adapting a contact-mechanics algorithm to predict damping in bolted joints using quasi-static modal analysis. *International Journal of Mechanical Sciences* 189: 105982. DOI:<https://doi.org/10.1016/j.ijmecsci.2020.105982>. URL <https://www.sciencedirect.com/science/article/pii/S0020740320303647>.